EUROPEAN JOURNAL OF COMPUTATIONAL MECHANICS, 2016
VOL. 25, NO. 4, 339–358
http://dx.doi.org/10.1080/17797179.2016.1212627

Taylor & Francis
Taylor & Francis Group

A Mindlin multilayered hybrid-mixed approach for shell structures without shear correction factors

Achraf Tafla[a], Wajdi Zouari[b] and Rezak Ayad[b]

[a]Department of Mechanical Engineering, Joya University Institute of Technology, Jouaiya, South Lebanon; [b]University of Reims Champagne-Ardenne, LISM EA 4695, IUT de Troyes, Troyes, France

ABSTRACT

In this paper, we present two four-node multilayered hybrid-mixed shell elements for the static and free vibration analyses of plate and shell composite structures. Their formulation is based on the first shear deformation theory of Reissner/Mindlin without transverse shear correction factors. Linear and quadratic variations of the local in-plane and transverse shear stresses across the thickness, respectively, are supposed. To reduce the total number of variables in these models, transverse shear stresses are directly related to bending stresses by using two equilibrium equations. The performances of the proposed elements are assessed by means of two known numerical benchmarks and their results are found to agree globally well with the reference solutions.

ARTICLE HISTORY
Received 1 June 2015
Accepted 11 July 2016

KEYWORDS
Laminated shells; finite element; natural hybrid-mixed model; FSDT; transverse shear; vibration

1. Introduction

To model thin and moderately thick plate and shell-like laminated composite structures, multilayered plate and shell finite elements have been developed for years (Carrera, 2002). The majority of these numerical tools adopt the first order shear deformation theory (FSDT) with transverse shear correction factors or higher order shear deformation theories (HSDT) without the need of these correction factors. The FSDT-based elements have the advantage to be simple to formulate and not too expensive in computing cost thanks to the first-order approximations commonly associated with the Reissner/Mindlin theory (Ayad, Talbi, & Ghomari, 2009; Brank & Carrera, 2000; Rolfes & Rohwer, 1997; Schürg, Wagner, and Gruttmann, 2009). Besides, the FSDT gives globally satisfactory results even for moderately thick laminates and is considered as the best compromise between accuracy and computing cost (Rohwer, 1992; Schürg et al., 2009). However, it is not always straightforward to calculate the shear correction factors which probably lead to erroneous results in some situations. To avoid using shear correction factors and obtain more accurate predictions of the stress field (especially transverse shear stresses), HSDT have been developed

CONTACT Achraf Tafla wajdi.zouari@univ-reims.fr

(Dhatt, 1969; Gay, 2005; Reddy, 1984, 1989; Topdar, Sheikh, & Dhang, 2003). For instance, Reddy (1984) considers a parabolic variation of the transverse shear strains across the thickness of the plate. Despite its accuracy, the main drawback of this type of formulation is the large number of variables per node which leads to highly computing costs especially when nonlinear problems are considered.

On the other hand, several mixed plate and shell finite elements have been also proposed to study multilayered composite structures as an alternative to displacement-based elements (Ayad et al., 2009; Bouabdallah, 1992; Carrera, 1996; Cen, Long, and Yao, 2002; Gruttmann & Wagner, 2006; Tafla, Ayad, and Sedira, 2010). For example, Carrera (1996) developed mixed multilayered plate elements that deliver accurate predictions of shear stresses within the laminate. Gruttmann and Wagner (2006) proposed a mixed-hybrid multilayered shell element based on a Hu-Washizu function with independent displacements, stress resultants and strains. Recently, Tafla et al. (2010) have proposed a FSDT mixed-hybrid multilayered four-node plate finite element, named MiSP4-ml, for the analysis of laminated and sandwich plates. The shear correction factors are avoided by using a quadratic approximation of the shear stresses across the thickness.

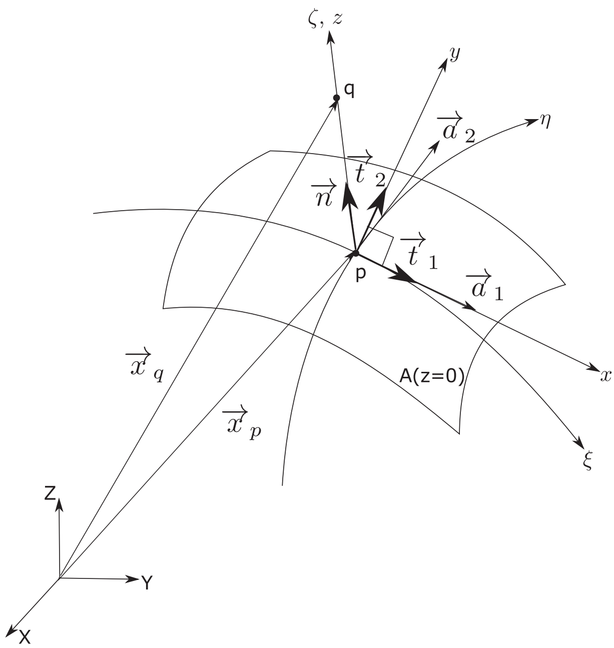

Figure 1. Geometry of a shell structure.

In this work, we propose an extension of the MiSP4-ml formulation to model shell composite structures. To this end, we adopt first, the 3D degenerated-solid approach to obtain the local curvilinear strains expressions (Batoz & Dhatt, 1992; Vlachoutsis, 1990). Then, a quadratic variation of the transverse shear stresses across the thickness is supposed to avoid using shear correction factors (Tafla et al., 2010). In order to reduce the total number of variables in the model, transverse shear stresses are directly related to bending stresses by using two equilibrium equations. For membrane stresses, two approaches are considered: in the first formulation, local membrane stresses are supposed to be directly related to curvilinear membrane strains through the membrane constitutive matrix which leads to the first shell element HMiSP4-Q4-ml, while for the second approach, membrane stresses are independently approximated as for bending and transverse shear stresses. This second formulation leads to the second developed multilayered shell element NHMiSP4-ml.

The present paper is structured as follows. In Section 2, we give the expressions of the local curvilinear strains based on the 3D degenerated-solid approach. Section 3 is devoted to the adopted mixed variational formulation based on the Reissner-Hellinger principle. In Section 4, we present the formulations of the proposed shell finite elements HMiSP4-Q4-ml and NHMiSP4-ml. Finally, the performance of the proposed multilayered shell elements is investigated by studying two static and free vibration benchmarks.

2. Gradient fields

2.1. Shell geometry

Consider a shell structure as depicted in Figure 1. Its geometry is characterized by a mid surface A considered as the reference surface and a constant thickness h. Let $\vec{x}_p(\xi, \eta)$ be the position vector of one point p of the reference surface in the global X, Y, Z coordinate system:

$$\vec{x}_p(\xi, \eta) = X_p(\xi, \eta)\,\vec{i} + Y_p(\xi, \eta)\,\vec{j} + Z_p(\xi, \eta)\,\vec{k} \tag{1}$$

At the reference surface A, the vectors of the covariant basis $[F_0] = [\vec{a}_1 \;\; \vec{a}_2 \;\; \vec{n}]$ are defined by:

$$\vec{a}_1 = \vec{x}_{p,\xi} \quad ; \quad \vec{a}_2 = \vec{x}_{p,\eta} \quad ; \quad \vec{n} = \frac{\vec{a}_1 \wedge \vec{a}_2}{\|\vec{a}_1 \wedge \vec{a}_2\|} \tag{2}$$

where $\vec{x}_{p,\alpha} = (\partial \vec{x}_p / \partial \alpha)$, $\alpha = \xi, \eta$. We introduce also the contravariant vectors $\vec{a}^{\,1}$ and $\vec{a}^{\,2}$ expressed in terms of the covariant vectors as:

$$\vec{a}^{\,1} \cdot \vec{a}_2 = \vec{a}^{\,2} \cdot \vec{a}_1 = 0 \quad \text{and} \quad \vec{a}^{\,1} \cdot \vec{a}_1 = \vec{a}^{\,2} \cdot \vec{a}_2 = 1 \tag{3}$$

In general, the covariant vectors are neither orthogonal nor unit vectors. Consequently, a new orthonormal basis $[Q] = [\vec{t}_1 \quad \vec{t}_2 \quad \vec{n}]$ is introduced at the reference surface to define the local curvilinear x, y, z coordinate system (Batoz & Dhatt, 1992):

$$[Q] = \begin{bmatrix} c + \frac{1}{1+c} n_Y^2 & -\frac{1}{1+c} n_X n_Y & n_X \\ -\frac{1}{1+c} n_X n_Y & c + \frac{1}{1+c} n_X^2 & n_Y \\ -n_X & -n_Y & n_Z \end{bmatrix} \quad \text{if} \quad 1 + c \neq 0 \tag{4}$$

and

$$[Q] = \begin{bmatrix} 1 & 0 & 0 \\ 0 & -1 & 0 \\ 0 & 0 & 1 \end{bmatrix} \quad \text{if} \quad 1 + c = 0 \tag{5}$$

where n_X, n_Y and n_Z are the global coordinates of the normal vector $\vec{n}$ and $c = \vec{n} \cdot \vec{k} = n_Z$.

At this stage, we introduce two matrices $[C_0]$ and $[b_c]$ whose components will be used in the curvilinear strains expressions in Section 2.3:

$$[C_0] = \begin{bmatrix} \vec{a}^1 \cdot \vec{t}_1 & \vec{a}^1 \cdot \vec{t}_2 \\ \vec{a}^2 \cdot \vec{t}_1 & \vec{a}^2 \cdot \vec{t}_2 \end{bmatrix} \quad ; \quad [b_c] = [\bar{b}][C_0] \quad \text{with} \quad [\bar{b}] = \begin{bmatrix} \vec{a}^2 \cdot \vec{n}_{,\eta} & -\vec{a}^1 \cdot \vec{n}_{,\eta} \\ -\vec{a}^2 \cdot \vec{n}_{,\xi} & \vec{a}^1 \cdot \vec{n}_{,\xi} \end{bmatrix} \tag{6}$$

$[C_0]$ permits to relate the curvilinear coordinates x and y to the natural coordinates ξ and η while $[\bar{b}]$ describes the warping of the reference surface. More details about these matrices can be found in Batoz and Dhatt (1992).

2.2. Mechanical displacement vector

Consider one point q of the shell structure located at the distance z from the mid surface A as depicted in Figure 1. The Reissner/Mindlin hypothesis permits to express the mechanical displacement vector of q in term of that of p:

$$\vec{u}_q(\xi, \eta, \zeta) = \vec{u}_p(\xi, \eta) + z\vec{\beta}(\xi, \eta) \quad ; \quad z = \frac{h}{2}\zeta \quad ; \quad \vec{\beta} = \vec{\theta} \wedge \vec{n} \quad ; \quad \vec{\beta} \cdot \vec{n} = 0 \tag{7}$$

$\vec{\theta}$ is the orthogonal rotation vector of $\vec{n}$ and can be written in the global and local curvilinear bases as:

$$\vec{\theta} = \theta_X \vec{i} + \theta_Y \vec{j} + \theta_Z \vec{k} = \theta_x \vec{t}_1 + \theta_y \vec{t}_2 \tag{8}$$

Thus,

$$\begin{Bmatrix} \theta_x \\ \theta_y \end{Bmatrix} = \begin{bmatrix} \langle t_1 \rangle \\ \langle t_2 \rangle \end{bmatrix} \begin{Bmatrix} \theta_X \\ \theta_Y \\ \theta_Z \end{Bmatrix} \tag{9}$$

The vector product $\vec{\beta} = \vec{\theta} \wedge \vec{n}$ leads to the following expression of $\vec{u}_q$:

$$\vec{u}_q(\xi, \eta, \zeta) = \vec{u}_p(\xi, \eta) + z\big(-\theta_x \vec{t}_2 + \theta_y \vec{t}_1\big) \tag{10}$$

where $\langle u_p \rangle = \langle U \quad V \quad W \rangle$ is the displacement vector of p in the global coordinate system.

2.3. Curvilinear strains

In-plane and transverse shear local curvilinear strains can be developed in term of the local thickness coordinate ζ as explained in Batoz and Dhatt (1992):

$$\{\varepsilon_s\} = \frac{1}{\mu(\zeta)}\Big(\{\varepsilon_0\} + \zeta\{\varepsilon_1\} + \zeta^2\{\varepsilon_2\}\Big) \quad ; \quad \{\gamma_s\} = \frac{1}{\mu(\zeta)}\Big(\{\gamma_0\} + \zeta\{\gamma_1\}\Big) \tag{11}$$

where

$$\langle \varepsilon_s \rangle = \langle \varepsilon_x \quad \varepsilon_y \quad \gamma_{xy} \rangle \quad ; \quad \langle \gamma_s \rangle = \langle \gamma_{xz} \quad \gamma_{yz} \rangle \quad ; \quad \gamma_{ij} = 2\,\varepsilon_{ij} \tag{12}$$

$\mu(\zeta)$ is expressed in terms of the mean curvature $2H$ and Gaussian curvature K as shown in Batoz and Dhatt (1992):

$$\mu(\zeta) = 1 - h\,\zeta H + \frac{h^2}{4}\zeta^2 K \tag{13}$$

In the following, simplified expressions of the curvilinear strains will be used because of the complexity of the mixed-hybrid formulation. Accordingly, we first neglect the mean and Gaussian curvatures in the expression of $\mu(\zeta)$ ($\mu(\zeta) \approx 1$) and second, suppose a linear variation of $\{\varepsilon_s\}$ and constant transverse shear strains γ_{xz} and γ_{xz} across the thickness. Accordingly, $\{\varepsilon_s\}$ and $\{\gamma_s\}$ are rewritten as:

$$\{\varepsilon_s\} = \{\varepsilon_0\} + \zeta\{\varepsilon_1\} \quad ; \quad \{\gamma_s\} = \{\gamma_0\} \tag{14}$$

where

$$\{\varepsilon_0\} = \begin{Bmatrix} \vec{t}_1 \cdot \vec{u}_{p,x} \\ \vec{t}_2 \cdot \vec{u}_{p,y} \\ \vec{t}_1 \cdot \vec{u}_{p,y} + \vec{t}_2 \cdot \vec{u}_{p,x} \end{Bmatrix} \quad ;$$
$$\{\varepsilon_1\} = \frac{h}{2}\begin{Bmatrix} \vec{t}_1 \cdot \vec{\beta}_{,x} + \vec{t}_1 \cdot \vec{\bar{u}}_{p,x} \\ \vec{t}_2 \cdot \vec{\beta}_{,y} + \vec{t}_2 \cdot \vec{\bar{u}}_{p,y} \\ \vec{t}_1 \cdot (\vec{\beta}_{,y} + \vec{\bar{u}}_{p,y}) + \vec{t}_2 \cdot (\vec{\beta}_{,x} + \vec{\bar{u}}_{p,x}) \end{Bmatrix} \tag{15}$$

and

$$\{\gamma_0\} = \begin{Bmatrix} \vec{t}_1 \cdot \vec{\beta} + \vec{n} \cdot \vec{u}_{p,x} \\ \vec{t}_2 \cdot \vec{\beta} + \vec{n} \cdot \vec{u}_{p,y} \end{Bmatrix} \tag{16}$$

Using the matrices $[C_0]$ and $[b_c]$ defined in Equation (6), $\vec{u}_{p,x}$, $\vec{u}_{p,y}$, $\vec{\bar{u}}_{p,x}$ and $\vec{\bar{u}}_{p,y}$ are given by:

$$\begin{cases} \vec{u}_{p,x} = C_{011}\vec{u}_{p,\xi} + C_{021}\vec{u}_{p,\eta} \\ \vec{u}_{p,y} = C_{012}\vec{u}_{p,\xi} + C_{022}\vec{u}_{p,\eta} \\ \vec{\bar{u}}_{p,x} = b_{c11}\vec{u}_{p,\xi} + b_{c21}\vec{u}_{p,\eta} \\ \vec{\bar{u}}_{p,y} = b_{c12}\vec{u}_{p,\xi} + b_{c22}\vec{u}_{p,\eta} \end{cases} \quad ; \quad C_{0ij} = C_0(i,j) \quad \text{and} \quad b_{cij} = b_c(i,j),\ i,j = 1,2 \tag{17}$$

3. Mixed-hybrid variational formulation

Consider a multilayered composite shell structure constituted of n_c layers. The weak form of its static equilibrium can be obtained by introducing the admissible virtual displacements $\vec{u}^{\,*}_q$ as:

$$W = W_{\text{int}} - W_{\text{ext}} = 0 \qquad \forall\ \vec{u}^{\,*}_q \quad \text{with} \quad \begin{cases} \vec{u}_q = \vec{U}_q \\ \vec{u}^{\,*}_q = \vec{0} \end{cases} \quad \text{on} \quad S_u \tag{18}$$

where W_{int} and W_{ext} are the internal and external virtual works, respectively, and S_u is the displacement boundary of the shell structure.
The internal virtual work W_{int} is written in a mixed-hybrid form and can be decomposed into a membrane-bending part W_{mf} and transverse shear part W_c as:

$$W_{mf} = \int_V \Big(\langle \varepsilon_s^* \rangle \{\sigma_s\} + \langle \sigma_s^* \rangle \{\varepsilon_s\} - \langle \sigma_s^* \rangle [H]^{-1} \{\sigma_s\} \Big) \mathrm{d}V \tag{19}$$

and

$$W_c = \int_V \Big(\langle \gamma_s^* \rangle \{\tau_s\} + \langle \tau_s^* \rangle \{\gamma_s\} - \langle \tau_s^* \rangle [G]^{-1} \{\tau_s\} \Big) \mathrm{d}V \tag{20}$$

with $\{\sigma_s\}$ and $\{\tau_s\}$ are the in-plane and transverse shear stress vectors ($\langle \sigma_s \rangle = \langle \sigma_x \quad \sigma_y \quad \sigma_{xy} \rangle$, $\langle \tau_s \rangle = \langle \sigma_{xz} \quad \sigma_{yz} \rangle$) and $[H]$ and $[G]$ are the local in-plane and out-of-plane elasticity matrices.
Linear and quadratic variations of $\{\sigma_s\}$ and $\{\tau_s\}$ across the thickness are supposed:

$$\{\sigma_s\} = \{\sigma_0\} + \zeta \{\sigma_1\} \quad ; \quad \{\tau_s\} = (1 - \zeta^2) \{\tau_0\} \tag{21}$$

where $\langle \sigma_0 \rangle = \langle \sigma_{x0} \quad \sigma_{y0} \quad \sigma_{xy0} \rangle$ and $\langle \sigma_1 \rangle = \langle \sigma_{x1} \quad \sigma_{y1} \quad \sigma_{xy1} \rangle$ are the membrane and bending curvilinear stress vectors, respectively, while $\langle \tau_0 \rangle = \langle \tau_{xz0} \quad \tau_{yz0} \rangle$ is the vector of curvilinear transverse shear stresses at the reference surface ($\zeta = 0$).
Using Equations (14) and (21), it is possible to explicitly integrate W_{mf} and W_c across the thickness. We obtain:

$$W_{mf} = \int_A \begin{pmatrix} h \langle \sigma_0^* \rangle \{\varepsilon_0\} + h \langle \varepsilon_0^* \rangle \{\sigma_0\} + \dfrac{h}{3} \langle \sigma_1^* \rangle \{\varepsilon_1\} + \\ \dfrac{h}{3} \langle \varepsilon_1^* \rangle \{\sigma_1\} - \langle \sigma_0^* \rangle [\overline{H}_m] \{\sigma_0\} - \langle \sigma_0^* \rangle [\overline{H}_{mf}] \{\sigma_1\} \\ - \langle \sigma_1^* \rangle [\overline{H}_{mf}]^T \{\sigma_0\} - \dfrac{h^4}{36} \langle \sigma_1^* \rangle [\overline{H}_f] \{\sigma_1\} \end{pmatrix} \mathrm{d}A \tag{22}$$

and

$$W_c = \int_A \left(\frac{2h}{3} \langle \gamma_0^* \rangle \{\tau_0\} + \frac{2h}{3} \langle \tau_0^* \rangle \{\gamma_0\} - \frac{h^2}{16} \langle \tau_0^* \rangle [\overline{H}_c] \{\tau_0\} \right) \mathrm{d}A \tag{23}$$

The new elasticity matrices $[\overline{H}_m]$, $[\overline{H}_{mf}]$, $[\overline{H}_f]$ and $[\overline{H}_c]$ traduce the multilayered aspect of the composite shell structure and are given by:

$$[\overline{H}_m] = \sum_{i=1}^{n_c} (z_{i+1} - z_i)[H]_i^{-1} \quad ; \quad [\overline{H}_{mf}] = \frac{1}{h} \sum_{i=1}^{n_c} (z_{i+1}^2 - z_i^2)[H]_i^{-1} \quad , \tag{24}$$

$$[\overline{H}_f] = \sum_{i=1}^{n_c} \left[\frac{(z_{i+1}^3 - z_i^3)}{3} [H]_i \right]^{-1} \tag{25}$$

$$[\overline{H}_c] = \sum_{i=1}^{n_c} \left((z_{i+1} - z_i) + \frac{16}{5h^4}(z_{i+1}^5 - z_i^5) - \frac{8}{3h^2}(z_{i+1}^3 - z_i^3) \right) [G]_i^{-1} \tag{26}$$

where z_i and z_{i+1} are the local coordinates of the ith layer across the thickness direction and $[H]_i$ and $[G]_i$ are its elastic matrices.
It is worthy to note that no shear correction factors are needed in the matrix $[\overline{H}_c]$ to model multilayered structures which is quite different from displacement-based models.

4. Finite element approximation

The solution of the weak form (18) can be obtained by the finite element method. The finite element approximation is constructed by dividing the composite shell structure into elementary domains. To this end, two four-node quadrilateral shell elements, named NHMiSP-ml and HMiSP4-Q$_4$-ml, were developed. For HMiSP4-Q$_4$-ml, the membrane stress vector $\{\sigma_0\}$ is directly related to $\{\varepsilon_0\}$ through $[H]$ ($\{\sigma_0\} = [H]\{\varepsilon_0\}$) while for NHMiSP-ml all stresses are interpolated independently of constitutive laws. Consequently, the membrane-bending part of the internal virtual work of HMiSP4-Q$_4$-ml reads:

$$W_{mf}^{\text{HMi-ml}} = \int_A \begin{pmatrix} \langle \varepsilon_0^* \rangle [H_m]\{\varepsilon_0\} + \langle \varepsilon_1^* \rangle [H_{mf}]\{\varepsilon_0\} + \langle \varepsilon_0^* \rangle [H_{mf}]^T \{\varepsilon_1\} + \\ \frac{h}{3} \langle \sigma_1^* \rangle \{\varepsilon_1\} + \frac{h}{3} \langle \varepsilon_1^* \rangle \{\sigma_1\} - \frac{h^4}{36} \langle \sigma_1^* \rangle [\overline{H}_f]\{\sigma_1\} \end{pmatrix} \mathrm{d}A \tag{27}$$

where

$$[H_m] = \sum_{i=1}^{n_c} (z_{i+1} - z_i)[H]_i \quad ; \quad [H_{mf}] = \frac{1}{h} \sum_{i=1}^{n_c} (z_{i+1}^2 - z_i^2)[H]_i \tag{28}$$

In the following, we give first, the finite element approximations of the membrane, bending and transverse shear strains and stresses and second, the stiffness and mass matrices expressions of NHMiSP-ml and HMiSP4-Q$_4$-ml.

4.1. Membrane and bending strains

The proposed shell elements are four-node quadrilateral elements (Figure 2). The bilinear shape function at node i is given as:

$$N_i(\xi, \eta) = \frac{1}{4}(1 + \xi_i \xi)(1 + \eta_i \eta) \qquad -1 \leq \xi, \eta \leq 1 \tag{29}$$

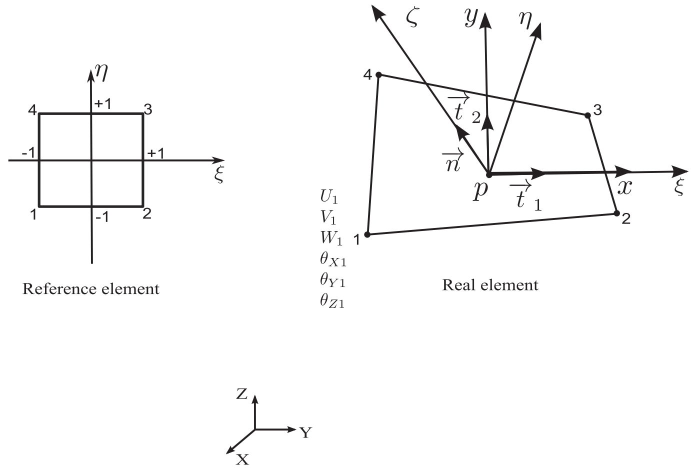

Figure 2. Four-node quadrilateral shell element.

These shape functions interpolate at the element level the displacement vector of p belonging to the reference surface and the rotation vector $\vec{\beta}$ to obtain (Batoz & Dhatt, 1992):

$$\vec{u_q} = \sum_{i=1}^{4} N_i \, \vec{U_i} + z \sum_{i=1}^{4} N_i \left(- \theta_{xi} \vec{t}_{2i} + \theta_{yi} \vec{t}_{1i} \right) \tag{30}$$

where $\langle U_i \rangle = \langle U_i \quad V_i \quad W_i \rangle$ is the displacement vector of node i in the global coordinate system and θ_{xi} and θ_{yi} are the rotations of the normal vector $\vec{n}_i$ around $\vec{t}_{1i}$ and $\vec{t}_{2i}$, respectively.

Based on Equations (15) and (30), we find the following approximations of $\{\varepsilon_0\}$ and $\{\varepsilon_1\}$:

$$\{\varepsilon_0\} = \underbrace{[B_0]}_{3\times 20} \{u_n^{\mathrm{loc}}\} \quad ; \quad [B_0] = \begin{bmatrix} \cdots & \langle t_1 \rangle \, N_{i,x} & 0 \; 0 & \\ & \langle t_2 \rangle \, N_{i,y} & 0 \; 0 & \cdots \; i = 1,4 \\ & \langle t_1 \rangle \, N_{i,y} + \langle t_2 \rangle \, N_{i,x} & 0 \; 0 & \end{bmatrix} \tag{31}$$

and

$$\{\varepsilon_1\} = \underbrace{[B_1]}_{3\times 20} \{u_n^{\mathrm{loc}}\} \tag{32}$$

with

$$[B_1] = \begin{bmatrix} \cdots & \langle t_1 \rangle \, \overline{N}_{i,x} & \frac{h}{2} \langle \bar{t}_{1i} \rangle \, N_{i,x} & \\ & \langle t_2 \rangle \, \overline{N}_{i,y} & \frac{h}{2} \langle \bar{t}_{2i} \rangle \, N_{i,y} & \cdots \; i = 1,4 \\ & \langle t_1 \rangle \, \overline{N}_{i,y} + \langle t_2 \rangle \, \overline{N}_{i,x} & \frac{h}{2} \left(\langle \bar{t}_{1i} \rangle \, N_{i,y} + \langle \bar{t}_{2i} \rangle \, N_{i,x} \right) & \end{bmatrix} \tag{33}$$

$N_{i,\alpha}$ and $\overline{N}_{i,\alpha}$, $\alpha = x, y$ are defined in terms of the components of the matrices $[C_0]$ and $[b_c]$ as in Equation (17). The vectors $\{\bar{t}_{1i}\}$ and $\{\bar{t}_{2i}\}$ are given by:

$$\langle \bar{t}_{1i} \rangle = \langle - \vec{t}_1 \cdot \vec{t}_{2i} \quad \vec{t}_1 \cdot \vec{t}_{1i} \rangle \quad ; \quad \langle \bar{t}_{2i} \rangle = \langle - \vec{t}_2 \cdot \vec{t}_{2i} \quad \vec{t}_2 \cdot \vec{t}_{1i} \rangle \tag{34}$$

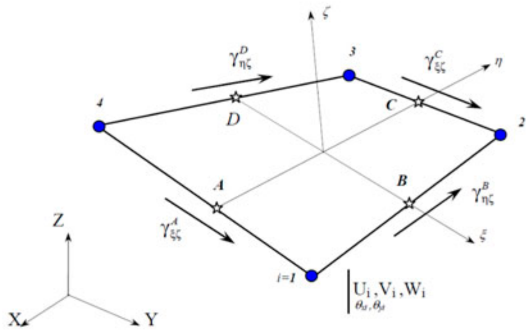

	ξ	η
A	0	-1
B	1	0
C	0	1
D	-1	0

Figure 3. Projection of the covariant transverse shear strains.

$\{u_n^{\text{loc}}\}$ is the local degrees of freedom vector of the proposed shell elements constituted of the global nodal displacements and local nodal rotations as:

$$\langle u_n^{\text{loc}} \rangle = \langle \cdots \quad U_i \ \ V_i \ \ W_i \ \ \theta_{xi} \ \ \theta_{yi} \quad \cdots i = 1, 4 \rangle \tag{35}$$

4.2. Transverse shear strains

To control transverse shear locking problems, an independent approximation of the shear strains is used. It's based on the Assumed Natural Strain projection technique proposed by Bathe and Dvorkin (1986).

Curvilinear $\langle \gamma_0 \rangle = \langle \gamma_{xz0} \quad \gamma_{yz0} \rangle$ and covariant $\langle \gamma_\zeta \rangle = \langle \gamma_{\xi\zeta} \quad \gamma_{\eta\zeta} \rangle$ transverse shear strains are related through the $[C_0]$ matrix as:

$$\{\gamma_0\} = [C_0]^T \{\gamma_\zeta\} \quad \Rightarrow \quad \{\gamma_\zeta\} = \begin{Bmatrix} \gamma_{\xi\zeta} \\ \gamma_{\eta\zeta} \end{Bmatrix} = \begin{Bmatrix} \vec{a}_1 \cdot \vec{\beta} + \vec{n} \cdot \vec{u}_{p,\xi} \\ \vec{a}_2 \cdot \vec{\beta} + \vec{n} \cdot \vec{u}_{p,\eta} \end{Bmatrix} \tag{36}$$

To avoid transverse shear locking, the middles of the quadrilateral element sides A, B, C and D (Figure 3) are considered to express the covariant transverse shear strains as:

$$\{\gamma_\zeta\} = [A]\{\gamma_{\zeta k}\} \quad ; \quad [A] = \frac{1}{2}\begin{bmatrix} 1-\eta & 0 & 1+\eta & 0 \\ 0 & 1+\xi & 0 & 1-\xi \end{bmatrix}, \quad \gamma_{\zeta k} = \begin{Bmatrix} \gamma_{\xi\zeta}^A \\ \gamma_{\eta\zeta}^B \\ \gamma_{\xi\zeta}^C \\ \gamma_{\eta\zeta}^D \end{Bmatrix} \tag{37}$$

It is possible to relate $\{\gamma_{\zeta k}\}$ to the local degrees of freedom vector $\{u_n^{\text{loc}}\}$ through a (4×20)-sized matrix $[B_{c\zeta}]$ as shown in Batoz and Dhatt (1992). In this case, we obtain the following approximation of the curvilinear transverse shear strains vector $\{\gamma_0\}$:

$$\{\gamma_0\} = \underbrace{[C_0]^T [A][B_{c\zeta}]}_{[B_c]}\{u_n^{\text{loc}}\} = \underbrace{[B_c]}_{2\times 20}\{u_n^{\text{loc}}\} \tag{38}$$

4.3. Membrane stresses

As discussed previously, the membrane curvilinear stresses of the multilayered shell element HMiSP4-Q_4-ml are directly related to the membrane strains as $\{\sigma_0\} = [H]\{\varepsilon_0\}$. Contrary to HMiSP4-$Q_4$-ml, the membrane stresses of NHMiSP4-ml are independently approximated of the membrane constitutive law. Accordingly, five membrane parameters $\alpha_{m1} \cdots \alpha_{m5}$ are used to approximate $\{\sigma_0\}$ as proposed by Pian and Sumihara (1984) and Ayad (2002):

$$\{\sigma_0\} = [P_0]\{\alpha_m\} \tag{39}$$

with

$$[P_0] = \frac{1}{c_0^2}\begin{bmatrix} C_{022}^2 & C_{012}^2 & -2C_{022}C_{012} & \eta C_{022}^2 & \xi C_{012}^2 \\ C_{021}^2 & C_{011}^2 & -2C_{021}C_{011} & \eta C_{021}^2 & \xi C_{011}^2 \\ -C_{022}C_{021} & -C_{012}C_{011} & C_{022}C_{011} + C_{012}C_{021} & -\eta C_{022}C_{021} & -\xi C_{012}C_{011} \end{bmatrix}$$

where $c_0 = \frac{h}{2}\det[C_0] = \frac{h}{2}\left(C_{011}C_{022} - C_{012}C_{021}\right)$. These parameters $\{\alpha_m\}$ are then eliminated by the static condensation technique performed locally at the element level.

4.4. Bending stresses

For the two developed multilayered shell elements, 12 parameters $\alpha_{f1} \cdots \alpha_{f12}$ are considered to estimate the vector of bending stresses $\{\sigma_1\}$:

$$\{\sigma_1\} = [P_1]\{\alpha_f\} \quad ; \quad [P_1] = \begin{bmatrix} \langle P\rangle & 0 & 0 \\ 0 & \langle P\rangle & 0 \\ 0 & 0 & \langle P\rangle \end{bmatrix} ; \quad \langle P\rangle = \langle 1 \;\; \xi \;\; \eta \;\; \xi\eta\rangle \tag{40}$$

These parameters $\{\alpha_f\}$ are also eliminated by the static condensation technique.

4.5. Transverse shear stresses

To limit the number of variables in the model, the approximation of the transverse shear stresses $\{\tau_0\}$ is directly derived from that of bending stresses $\{\sigma_1\}$ given in Equation (40). To this end, we consider the following static equilibrium equations:

$$\begin{aligned} \sigma_{x,x} + \tau_{xy,y} + \tau_{xz,z} + f_x = 0 \\ \tau_{xy,x} + \sigma_{y,y} + \tau_{yz,z} + f_y = 0 \end{aligned} \tag{41}$$

where f_x and f_y are the body force densities along x and y. As explained in Ayad (2002), $\{\tau_0\}$ is found to be related to the divergence of the the membrane stress tensor $[\sigma_1]$ when Equation (41) are integrated across the thickness direction:

$$\{\tau_0\} = \frac{h}{4}\mathrm{div}[\sigma_1] \quad ; \quad [\sigma_1] = \begin{bmatrix} \sigma_{1x} & \sigma_{1xy} \\ \sigma_{1xy} & \sigma_{1y} \end{bmatrix} \tag{42}$$

Consequently, we obtain

$$\{\tau_0\} = \frac{h}{4}\left\{\begin{matrix}\sigma_{1x,x} + \tau_{1xy,y} \\ \tau_{1xy,x} + \sigma_{1y,y}\end{matrix}\right\} = \underbrace{\frac{h}{4}[P_s]}_{[P_\tau]}\{\alpha_f\} \quad ; \quad [P_s] = \begin{bmatrix}\langle P_1\rangle & 0 & \langle P_2\rangle \\ 0 & \langle P_2\rangle & \langle P_1\rangle\end{bmatrix} \tag{43}$$

where

$$\langle P_1\rangle = \langle 0 \;\; j_{11} \;\; j_{12} \;\; \eta j_{11} + \xi j_{12}\rangle \quad ; \quad \langle P_2\rangle = \langle 0 \;\; j_{21} \;\; j_{22} \;\; \eta j_{21} + \xi j_{22}\rangle \tag{44}$$

and j_{kl} are the components of the Jacobian matrix inverse.

4.6. Stiffness matrices of HMiSP4-Q$_4$-ml and NHMiSP4-ml

For the first shell element HMiSP4-Q$_4$-ml, the bending and transverse shear stresses approximations in terms of the parameters $\{\alpha_f\}$ lead to the following final expression of the internal virtual work:

$$W_{\mathrm{int}}^{\mathrm{HMi\text{-}ml}} = \langle\langle\alpha_f^*\rangle \;\; \langle u_n^{\mathrm{loc}\,*}\rangle\rangle \begin{bmatrix}-[K_1] & [K_{1u}] \\ [K_{1u}]^T & [K_0]\end{bmatrix}\left\{\begin{matrix}\{\alpha_f\} \\ \{u_n^{\mathrm{loc}}\}\end{matrix}\right\} \tag{45}$$

where

$$\underbrace{[K_0]}_{20\times 20} = \int_A [B_0]^T[H_m][B_0]\,\mathrm{d}A + \int_A [B_1]^T[H_{mf}][B_0]\,\mathrm{d}A + \int_A [B_0]^T[H_{mf}][B_1]\,\mathrm{d}A \tag{46}$$

$$\underbrace{[K_1]}_{12\times 12} = \frac{h^4}{36}\int_A [P_1]^T[\overline{H}_f][P_1]\,\mathrm{d}A + \frac{h^2}{16}\int_A [P_\tau]^T[\overline{H}_c][P_\tau]\,\mathrm{d}A \tag{47}$$

$$\underbrace{[K_{1u}]}_{12\times 20} = \frac{h^2}{6}\int_A [P_\tau]^T[B_c]\,\mathrm{d}A + \frac{h}{3}\int_A [P_1]^T[B_1]\,\mathrm{d}A \tag{48}$$

After static condensation of the parameters $\{\alpha_f\}$, the final local stiffness matrix of the multilayered shell element HMiSP4-Q$_4$-ml is written as:

$$\underbrace{[K^{\mathrm{HMiSP4\text{-}Q_4\text{-}ml}}]}_{20\times 20} = [K_0] + [K_{1u}]^T[K_1]^{-1}[K_{1u}] \tag{49}$$

For the second multilayered shell element NHMiSP4-ml, the approximations of membrane, bending and transverse shear stresses in terms of the parameters $\{\alpha_m\}$ and $\{\alpha_f\}$ lead to the following expression of the internal virtual work:

$$W_{\mathrm{int}}^{\mathrm{NHMi\text{-}ml}} = \langle\langle\alpha_m^*\rangle \;\; \langle\alpha_f^*\rangle \;\; \langle u_n^{\mathrm{loc}\,*}\rangle\rangle \begin{bmatrix}-[K_{mm}] & [K_{mf}] & [K_{mu}] \\ [K_{mf}]^T & -[K_f] & [K_{fu}] \\ [K_{mu}]^T & [K_{fu}]^T & [0]\end{bmatrix}\left\{\begin{matrix}\{\alpha_m\} \\ \{\alpha_f\} \\ \{u_n^{\mathrm{loc}}\}\end{matrix}\right\} \tag{50}$$

where

$$\underbrace{[K_{mm}]}_{5\times 5} = \int_A [P_0]^T[\overline{H}_m][P_0]\,\mathrm{d}A \quad ; \quad \underbrace{[K_{mu}]}_{5\times 20} = h\int_A [P_0]^T[B_0]\,\mathrm{d}A \tag{51}$$

$$\underbrace{[K_f]}_{12\times 12} = \frac{h^4}{36}\int_A [P_1]^T[\overline{H}_f][P_1]\,\mathrm{d}A + \frac{h^2}{16}\int_A [P_\tau]^T[\overline{H}_c][P_\tau]\,\mathrm{d}A \tag{52}$$

$$\underbrace{[K_{fu}]}_{12\times 20} = \frac{h^2}{6}\int_A [P_\tau]^T[B_c]\,\mathrm{d}A + \frac{h}{3}\int_A [P_1]^T[B_1]\,\mathrm{d}A \quad ; \underbrace{[K_{mf}]}_{5\times 20} = \int_A [P_0]^T[\overline{H}_{mf}][P_1]\,\mathrm{d}A \tag{53}$$

After static condensation of the parameters $\{\alpha_m\}$ and $\{\alpha_f\}$, the final local stiffness matrix of the multilayered shell element NHMiSP4-ml is written as:

$$\underbrace{[K^{\text{NHMiSP4-ml}}]}_{20\times 20} = [A_1] + [A_2][A_3]^{-1}[A_2]^T \tag{54}$$

with

$$[A_1] = [K_{fu}]^T + [K_{mu}]^T[K_{mm}]^{-1}[K_{mu}] \tag{55}$$

$$[A_2] = [K_{mu}]^T[K_{mm}]^{-1}[K_{mf}] \quad ; \quad [A_3] = [K_{mf}]^T[K_{mm}]^{-1}[K_{mf}] \tag{56}$$

Finally, it is worthy to note that 2×2 Gauss points are sufficient to exactly integrate the stiffness matrices of HMiSP4-Q$_4$-ml and NHMiSP4-ml.

4.7. Virtual stiffness matrix

When passing from the local to the global coordinate system, we introduce a fictive work W_{θ_z} associated with the local rotation θ_z to avoid the singularity of the global stiffness matrix as proposed in Batoz and Dhatt (1992):

$$W_{\theta_z} = \int_A \alpha H_{f11}\left(\theta^*_{z,x}\theta_{z,x} + \theta^*_{z,y}\theta_{z,y}\right)\mathrm{d}A \tag{57}$$

where $H_{f11} = \overline{H}_f(1,1)$ and α is a very small numerical coefficient ($\alpha = 10^{-6}$). With the approximation $\theta_z = \sum_{i=1}^4 N_i(\xi,\eta)\ \theta_{zi}$, it is possible to write W_{θ_z} in term of a new (4×4)-sized fictive stiffness matrix $[k_{\theta z}]$ as:

$$W_{\theta_z} = \langle \theta^*_{z1}\ \theta^*_{z2}\ \theta^*_{z3}\ \theta^*_{z4}\rangle \begin{bmatrix} k_{\theta z11} & 0 & 0 & 0 \\ 0 & k_{\theta z22} & 0 & 0 \\ 0 & 0 & k_{\theta z33} & 0 \\ 0 & 0 & 0 & k_{\theta z44} \end{bmatrix} \begin{Bmatrix} \theta_{z1} \\ \theta_{z2} \\ \theta_{z3} \\ \theta_{z4} \end{Bmatrix} \tag{58}$$

To transform the local (20 × 20)-sized stiffness matrices of the proposed shell elements into the global coordinate system, the following passage matrix is used:

$$\underbrace{[T]}_{24\times 24} = \begin{bmatrix} [I_3] & & & & \\ & [Q_1] & & & \\ & & \ddots & & \\ & & & [I_3] & \\ & & & & [Q_4] \end{bmatrix} \tag{59}$$

where $[I_3]$ is the identity matrix of size 3 and $[Q_1]\ldots[Q_4]$ are the nodal tangent curvilinear bases. We write

$$[K^{\text{glob}}] = [T][K^{\text{loc}}][T]^T \tag{60}$$

where $[K^{\text{loc}}]$ is obtained from $[K^{\text{HMiSP4-Q}_4\text{-ml}}]$ or $[K^{\text{NHMiSP4-ml}}]$ by adding the components of the fictive stiffness matrix $[k_{\theta z}]$ as:

$$[K^{\text{loc}}] = \begin{bmatrix} \ddots & & \\ & \underbrace{[K_i]}_{5\times 5} & \{0\} \\ & \langle 0\rangle & k_{\theta zii} \\ & & & \ddots \end{bmatrix} \quad i = 1,4 \tag{61}$$

4.8. *Effective mass matrix of the multilayered shell elements*

In this section, we give the expression of the mass matrix of the proposed multilayered shell elements to study free vibrations of shell composite structures. At the element level, the kinetic energy is written as:

$$V = \frac{1}{2}\int_{V^e} \rho\left(\dot{\vec{u}}_q \cdot \dot{\vec{u}}_q\right) \mathrm{d}V \quad ; \quad \dot{\vec{u}}_q = \frac{d\vec{u}_q}{\mathrm{d}t} \tag{62}$$

where ρ is the mass density of the composite material defined at each layer. $\vec{u}_q$ is written in term of $\vec{u}_p$ and $\vec{\theta}$ as:

$$\vec{u}_q = \vec{u}_p + z\vec{\theta} \wedge \vec{n} = U\vec{i} + V\vec{j} + W\vec{k} + z(-\theta_x \vec{t}_2 + \theta_y \vec{t}_1) \tag{63}$$

The expression of $\vec{u}_q$ could be rewritten in the following simplified expression:

$$\vec{u}_q = (U + z\theta_r(1))\vec{i} + (V + z\theta_r(2))\vec{j} + (W + z\theta_r(3))\vec{k} \tag{64}$$

with

$$\theta_r(1) = -\theta_x t_{2X} + \theta_y t_{1X} \quad ; \quad \theta_r(2) = -\theta_x t_{2Y} + \theta_y t_{1Y} \quad ; \quad \theta_r(3) = -\theta_x t_{2Z} + \theta_y t_{1Z} \tag{65}$$

Substituting Equation (64) into Equation (62), the kinetic energy is rewritten as:

$$\begin{aligned} V = & \frac{1}{2}\int_{V^e} \rho\left(\dot{U}\dot{U} + \dot{V}\dot{V} + \dot{W}\dot{W}\right) \mathrm{d}V \\ & + \frac{1}{2}\int_{V^e} \rho\, z \left(2\dot{U}\dot{\theta}_r(1) + 2\dot{V}\dot{\theta}_r(2) + 2\dot{W}\dot{\theta}_r(3)\right) \mathrm{d}V \\ & + \frac{1}{2}\int_{V^e} \rho\, z^2 \left(\dot{\theta}_r^2(1) + \dot{\theta}_r^2(2) + \dot{\theta}_r^2(3)\right) \mathrm{d}V \end{aligned} \tag{66}$$

The following approximations are used to obtain the local mass matrix expression:

$$\begin{array}{l} \dot{U} = \langle N_u\rangle\{\dot{u}_n^{\mathrm{loc}}\} \quad ; \quad \dot{V} = \langle N_v\rangle\{\dot{u}_n^{\mathrm{loc}}\} \quad ; \quad \dot{W} = \langle N_w\rangle\{\dot{u}_n^{\mathrm{loc}}\} \\ \dot{\theta}_r(1) = \langle N_{r_1}\rangle\{\dot{u}_n^{\mathrm{loc}}\} \quad ; \quad \dot{\theta}_r(2) = \langle N_{r_2}\rangle\{\dot{u}_n^{\mathrm{loc}}\} \quad ; \quad \dot{\theta}_r(2) = \langle N_{r_3}\rangle\{\dot{u}_n^{\mathrm{loc}}\} \end{array} \tag{67}$$

We write finally

$$V = \frac{1}{2}\langle \dot{u}_n^{\mathrm{loc}}\rangle[M]\{\dot{u}_n^{\mathrm{loc}}\} \tag{68}$$

with

$$[M] = \int_A \begin{bmatrix} c_1\Big(\{N_u\}\langle N_u\rangle + \{N_v\}\langle N_v\rangle + \{N_w\}\langle N_w\rangle\Big)+ \\ 2c_2\Big(\{N_u\}\langle N_{r_1}\rangle + \{N_v\}\langle N_{r_2}\rangle + \{N_w\}\langle N_{r_3}\rangle\Big)+ \\ c_3\Big(\{N_{r_1}\}\langle N_{r_1}\rangle + \{N_{r_2}\}\langle N_{r_2}\rangle + \{N_{r_3}\}\langle N_{r_3}\rangle\Big) \end{bmatrix} \mathrm{d}A$$

and

$$c_1 = \sum_{i=1}^{n_c} \rho_i(z_{i+1} - z_i) \quad ; \quad c_2 = \frac{1}{2}\sum_{i=1}^{n_c} \rho_i(z_{i+1}^2 - z_i^2) \quad ; \quad c_3 = \frac{1}{3}\sum_{i=1}^{n_c} \rho_i(z_{i+1}^3 - z_i^3) \tag{69}$$

5. Numerical validation examples

In this section, two static and free vibration benchmarks are considered to assess the efficiency and accuracy of the proposed multilayered shell elements.

5.1. Composite cylindrical panel under doubly sinusoidal loading

We consider in this example a simply-supported cylindrical panel subjected to a sinusoidal loading $q = q_0 \sin(\pi Y/L)\sin(\pi\theta/\phi)$ ($\phi = \pi/3$ and $L = 30$) as shown in Figure 4. It is composed of three layers [90/0/90], whose properties are summarized in Figure 4, with three slenderness ratios $R/h = 5$, 10 and 20. Thanks to the problem symmetry, only one-fourth of the cylindrical panel

Table 1. The simply-supported composite cylindrical panel. Normalized transverse displacement of point C.

R/h	NHMiSP4-ml (8 × 8)	NHMiSP4-ml (20 × 20)	HMiSP4-Q4-ml (8 × 8)	HMiSP4-Q4-ml (20 × 20)	EHOST (16 × 20) (Cho & Kim, 2000)	Reference (Varadan & Bhaskar, 1991)
5	3.221	3.284	3.122	3.425	3.862	3.694
10	1.247	1.421	1.333	1.512	1.579	1.578
20	.821	.922	.923	1.013	1.012	1.017

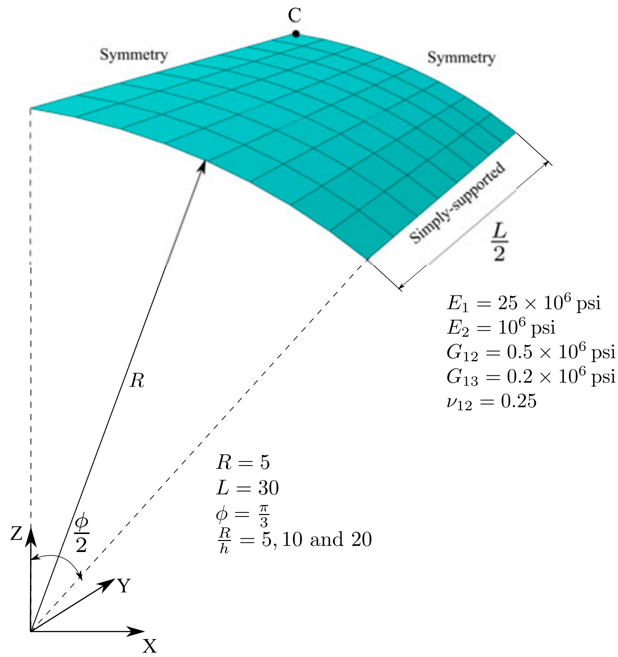

Figure 4. Simply-supported composite cylindrical panel meshed with 8 $\times$ 8 quadrilateral shell elements.

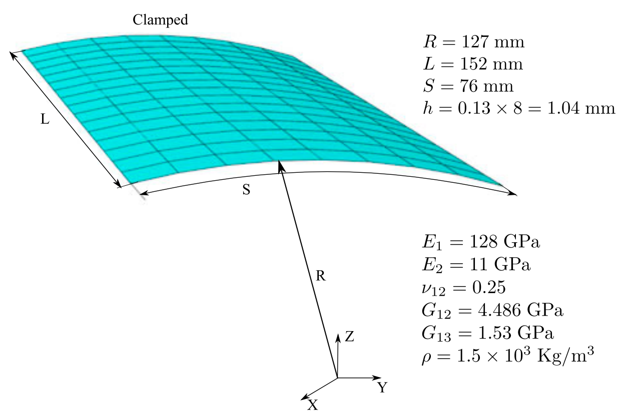

Figure 5. Cantilever composite panel meshed with 8 $\times$ 16 quadrilateral shell elements.

is considered and modeled with two regular meshes 8 $\times$ 8 and 20 $\times$ 20. We summarize in Table 1 the normalized transverse displacement at point C located at the center of the composite panel defined by:

$$\overline{W}_C = \frac{100\, E_1}{q_0\, S^4\, h} W_C \quad ; \quad S = \frac{R}{h} \tag{70}$$

The results of NHMiSP4-ml and HMiSP4-Q4-ml are compared first, with the elastic analytical solution of Varadan and Bhaskar reported in Varadan and

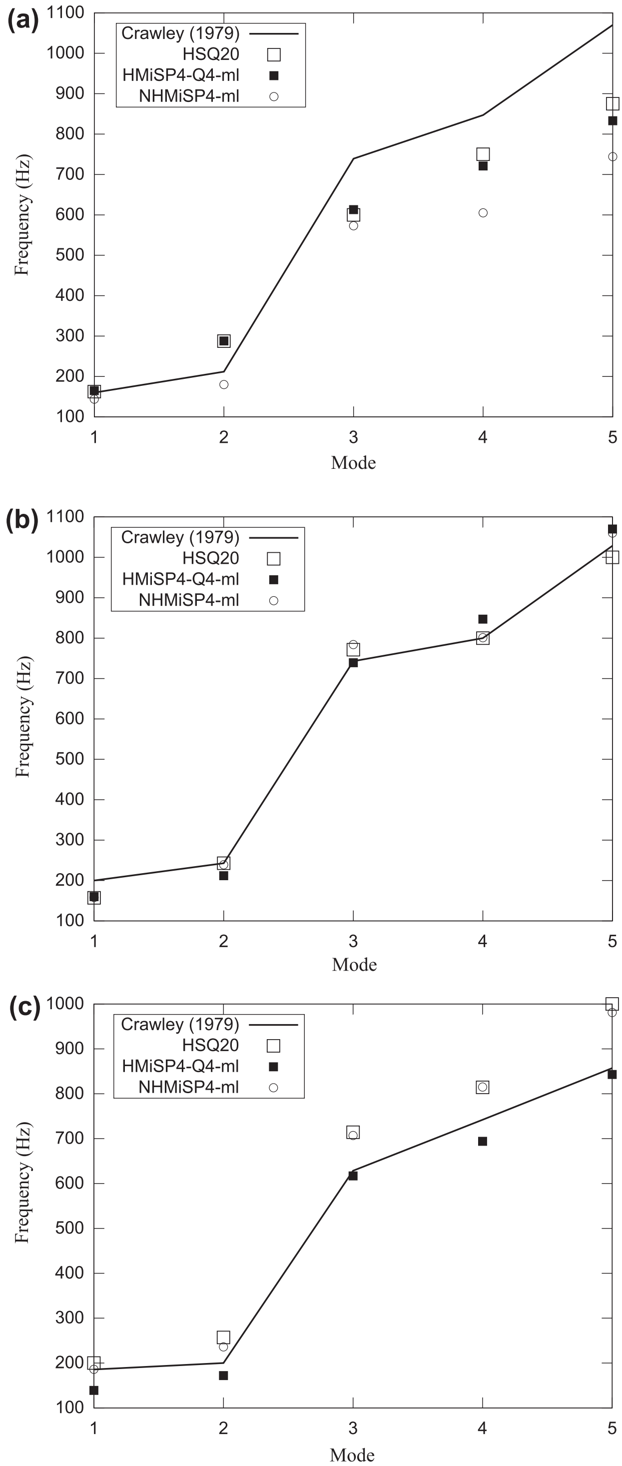

Figure 6. Natural frequencies of the clamped composite panels: (a) $[0_2/\pm30]_S$, (b) $[\pm45]_{2S}$ and (c) $[0/\pm45/90]$.

Bhaskar (1991) and second, with the element EHOST (Cho & Kim, 2000) (EHOST is a doubly curved nine-node shell element). We remark that NHMiSP4-ml and HMiSP4-Q4-ml agree globally well with the reference solution of Varadan and Bhaskar (1991). NHMiSP4-ml is found to be slightly less accurate than HMiSP4-Q4-ml. The NHMiSP4-ml result remains stable when the slenderness ratio is increased (at each case, approximately 90% of the reference result is reached with the second regular mesh 20 $\times$ 20). We remark also that HMiSP4-Q4-ml become more accurate when the slenderness ratio increases (92.7% of the reference displacement is reached for $R/h = 5$ and 99.6% for $R/h = 20$ with the second mesh).

5.2. Free vibration analysis of composite panels

This example was proposed by Crawley (1979) and concerns the study of free vibrations of three eight-layered carbon/epoxy composite cylindrical panels presenting the same dimensions with three stacking sequences: $[0_2/\pm 30]_S$, $[\pm 45]_{2S}$ and $[0/\pm 45/90]_S$. Figure 5 depicts the geometry and material properties of the clamped cylindrical panels and the 8 $\times$ 16 regular mesh used to model them. In particular, we will be interested in the first five natural modes and frequencies of these composite panels. We show in Figure 6 the obtained results of NHMiSP4-ml and NHMiSP4-Q4-ml compared to the experimental results of Crawley (1979) and the results of the element HSQ20 developed by Bouabdallah (1992) (HSQ20 is a four-node quadrilateral shell element having five degrees of freedom per node).

Except for the first composite panel $[0_2/\pm 30]_S$, NHMiSP4-ml and NHMiSP4-Q4-ml results agree globally well with the experimental frequencies of Crawley (1979). For the third composite panel $[0/\pm 45/90]$, NHMiSP4-Q4-ml is found to be the most accurate element.

6. Conclusion

In this paper, two hybrid-mixed multilayered shell finite elements, named NHMiSP4-ml and HMiSP4-Q4-ml, were eveloped to deal with static and free vibration analyses of laminated composite plate and shell structures. Their formulation is based on the Reissner/Mindlin FSDT without using the classical shear correction factors. For NHMiSP4-ml, membrane, bending and transverse shear stresses are interpolated independently of constitutive laws while for HMiSP4-Q4-ml, only bending and transverse shear stresses are independently approximated. Two static and free vibration dynamic numerical benchmarks were considered as validation tests and the results of the proposed shell elements were shown to agree globally well with the reference solutions.

Disclosure statement

No potential conflict of interest was reported by the authors.

References

Ayad, R. (2002). *Contribution to the numerical modeling of solids and structures and the non-newtonian fluids forming process. Application to packaging materials* (in French). Reims: Habilitation to conduct researches, University of Reims.

Ayad, R., Talbi, N., & Ghomari, T. (2009). Modified discrete Mindlin hypothesises for laminated composite structures. *Composites Science and Technology, 69*, 125–128.

Bathe, K. J., & Dvorkin, E. N. (1986). A formulation of general shell elements the use of mixed interpolation of tensorial components. *International Journal for Numerical Methods in Engineering, 22*, 697–722.

Batoz, J., & Dhatt, G. (1992). *Modélisation des structures par éléments finis* (Volume 3) [Modeling of Structures by finite elements, Volume 3: Shells (in French)]. Coques: Hermes.

Bouabdallah, M. S. (1992). Modélisation de coques cylindriques raidies, isotropes et composites (PhD thesis) [Modeling of stiffened, isotropic and composite cylindrical shells (in French) PhD thesis]. University of Technology of Compiègn, France.

Brank, B., & Carrera, E. (2000). Multilayered shell finite element with interlaminar continuous shear stresses: A refinement of the Reissner–Mindlin formulation. *International Journal for Numerical Methods in Engineering, 48*, 843–874.

Carrera, E. (1996). C^0 Reissner–Mindlin multilayered plate elements including zig-zag and interlaminar stress continuity. *International Journal for Numerical Methods in Engineering, 39*, 1797–1820.

Carrera, E. (2002). Theories and finite elements for multilayered, anisotropic, composite plates and shells. *Archives of Computational Methods in Engineering, 9*, 87–140.

Cen, S., Long, Y., & Yao, Z. (2002). A new hybrid-enhanced displacement-based element for the analysis of laminated composite plates. *Computers and Structures, 80*, 819–833.

Cho, M., & Kim, J. S. (2000). A postprocess method for laminated shells with a doubly curved nine-noded finite element. *Composites Part B: Engineering, 31*, 65–74.

Crawley, E. F. (1979). The natural modes of graphite/epoxy cantilever plates and shells. *Journal of Composite Materials, 13*, 195–205.

Dhatt, G. (1969). Numerical analysis of thin shells by curved triangular elements based on discrete kirchoff hypothesis. In *Pro-ceedings of the ASCE symposium on applications of FEM in civil engineering* (pp. 255–275). Nashville, TN: Vanderbilt University.

Gay, D. (2005). *Matériaux composites* [Composite Materials (in French)]. Lavoisier.

Gruttmann, F., & Wagner, W. (2006). Structural analysis of composite laminates using a mixed hybrid shell element. *Computational Mechanics, 37*, 479–497.

Pian, T. H. H., & Sumihara, K. (1984). Rational approach for assumed stress finite elements. *International Journal for Numerical Methods in Engineering, 20*, 1685–1695.

Reddy, J. N. (1984). A simple high-order theory for laminated composite plates. *Journal of Applied Mechanics, 51*, 745–752.

Reddy, J. N. (1989). On refined computational models of composite laminates. *International Journal for Numerical Methods in Engineering, 27*, 361–382.

Rohwer, K. (1992). Application of higher order theories to the bending analysis of layered composite plates. *International Journal of Solids and Structures, 29*, 105–119.

Rolfes, R., & Rohwer, K. (1997). Improved transverse shear stresses in composite finite elements based on first order shear defromation theory. *International Journal for Numerical Methods in Engineering, 40*, 51–60.

Schürg, M., Wagner, W., & Gruttmann, F. (2009). An enhanced FSDT model for the calculation of interlaminar shear stresses in composite plate structures. *Computational Mechanics, 44*, 765–776.

Tafla, A., Ayad, R., & Sedira, L. (2010). A Mindlin multilayered hybrid-mixed approach for laminated and sandwich structures without shear correction factors. *European Journal of Computational Mechanics, 19*, 725–742.
Topdar, P., Sheikh, A. H., & Dhang, N. (2003). Finite element analysis of composite and sandwich plates using a continuous inter-laminar shear stress model. *Journal of Sandwich Structures and Materials, 5*, 207–231.
Varadan, T. K., & Bhaskar, K. (1991). Bending of laminated orthotropic cylindrical shells – An elasticity approach. *Composite Structures, 17*, 141–156.
Vlachoutsis, S. (1990). Explicit integration for three-dimensional degenerated shell finite elements. *International Journal for Numerical Methods in Engineering, 29*, 861–880.